

Safe and Durable High-Temperature Lithium–Sulfur Batteries via Molecular Layer Deposited Coating

Xia Li,[†] Andrew Lushington,[†] Qian Sun,[†] Wei Xiao,^{†,‡} Jian Liu,^{†,‡} Biqiong Wang,^{†,‡} Yifan Ye,[‡] Kaiqi Nie,[‡] Yongfeng Hu,[§] Qunfeng Xiao,[§] Ruying Li,[†] Jinghua Guo,[‡] Tsun-Kong Sham,[†] and Xueliang Sun^{*,†}

[†]Department of Mechanical and Materials Engineering, University of Western Ontario, London, Ontario N6A 5B9, Canada

[‡]Advanced Light Source, Lawrence Berkeley National Laboratory, MS6R2100, One Cyclotron Road, Berkeley, California 94720, United States

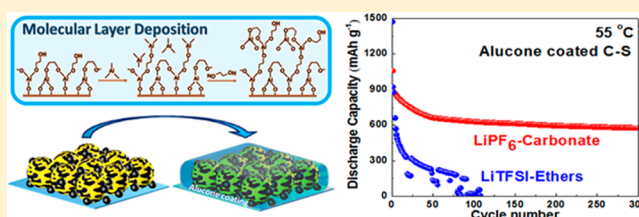
[§]Canadian Light Source, 44 Innovation Boulevard, Saskatoon, Saskatchewan S7N 2 V3, Canada

[‡]Department of Chemistry, University of Western Ontario, London, Ontario N6A 5B7, Canada

S Supporting Information

ABSTRACT: Lithium–sulfur (Li–S) battery is a promising high energy storage candidate in electric vehicles. However, the commonly employed ether based electrolyte does not enable to realize safe high-temperature Li–S batteries due to the low boiling and flash temperatures. Traditional carbonate based electrolyte obtains safe physical properties at high temperature but does not complete reversible electrochemical reaction for most Li–S batteries. Here we realize safe high temperature Li–S batteries on universal carbon–sulfur electrodes by molecular layer deposited (MLD) alucone coating. Sulfur cathodes with MLD coating complete the reversible electrochemical process in carbonate electrolyte and exhibit a safe and ultrastable cycle life at high temperature, which promise practicable Li–S batteries for electric vehicles and other large-scale energy storage systems.

KEYWORDS: Lithium–sulfur batteries, molecular layer deposition, MLD, high temperature, carbonate based electrolyte, ether based electrolyte



Lithium–sulfur battery is an attractive energy storage system due to the ultrahigh theoretical energy density and therefore considered as a promising energy device to meet the growing energy demands for high power output applications such as electric vehicles (EVs) and hybrid electric vehicles (HEVs).^{1,2} From a practical and industrial perspective, a critical requirement of batteries in EVs and HEVs is safe operation with a wide temperature window.^{3,4} Unfortunately, state-of-the-art ether based electrolytes for Li–S batteries suffer from low boiling and flash points (Table S1), and therefore pose significant safety risks for operation at elevated temperatures. In addition, the commonly used LiNO₃ additive is an oxidizing agent and provides further safety concerns.^{5,6} Moreover, high temperatures also promote lithium polysulfide dissolution into the electrolyte, resulting in poor cycle life.^{7,8} These safety concerns have considerably restricted the potential application of Li–S batteries in EVs with the use of ether based electrolyte and may involve the redesignation of sulfur cathodes in practical applications.^{9–12}

One possible solution in addressing these temperature issues for Li–S batteries is revisiting the use of traditional carbonate based Li-ion electrolytes, which have been developed and adopted for lithium-ion batteries (LIBs) over three decades.^{13–15} Unfortunately, attempts in employing carbonate based electrolytes for Li–S batteries were rarely succeeded

due to side reactions between carbonate solvents and electrochemical intermediates such as lithium polysulfide species, resulting in the irreversible electrochemical behavior of batteries.^{13–15} Very recently, a possible approach has been developed to solve this issue by capturing sulfur within fine holes tailored into carbon hosts.^{16,17} The confined sulfur molecules undergo solid-state electrochemical conversion to avoid solution based side reactions. However, it still needs specially manufactured microporous carbon–sulfur composites, which requires delicate control in laboratory-scale fabrication. Thereby, a critical question now arises: Is there a simple and versatile approach to be used in sulfur cathodes with carbonate based electrolytes to realize the safe operation of Li–S batteries at high temperature?

Atomic layer deposition (ALD) and molecular layer deposition (MLD) have gained considerable attention as ideal ultrathin-film techniques for the applications in energy storage systems.^{18–21} With self-limiting binary reactions, MLD demonstrates unparalleled advantages in producing uniform and conformal thin films, providing precise and flexible control over film thickness and chemical composition of the target

Received: February 9, 2016

Revised: May 2, 2016

Published: May 13, 2016

material at a molecular scale.^{20,21} Furthermore, the introduction of organic precursors during the deposition process enables the synthesis of hybrid metal–polymeric thin films. Up to now, ALD and MLD have been used to produce protective coating materials, solid-state electrolytes, and electrode materials for Li-based batteries to improve their cycle life and safety.^{21–23}

In this report, we propose a novel strategy to enable the use of carbonate-based electrolyte with universal carbon–sulfur electrodes of secondary Li–S batteries by MLD. Instead of elaborately designed microporous carbon, commercially available mesoporous carbon is employed as a sulfur host to demonstrate the universal application of MLD. The MLD alucone thin film material we employed in this research has demonstrated desirable flexible mechanical properties as a coating material for Li-ion and Li–S batteries, exhibiting solid and prolonged protection for electrodes during cycling.^{23,24} Furthermore, a number of excellent papers have demonstrated the use of ALD Al_2O_3 coating for sulfur cathodes, demonstrating improved cycle performance as well as stabilized and prolonged cycle life for Li–S batteries.^{25,26} The MLD alucone film in this report acts as an effective protecting layer and enables a reversible charge/discharge behavior for carbon–sulfur electrodes in carbonate-based electrolytes by preventing side reactions from occurring between sulfide/polysulfide intermediates and carbonate solvents. With the MLD coated carbon–sulfur electrodes, we demonstrate that high temperature Li–S batteries have safe and stable ultralong cycle life operating in carbonate-based electrolyte. Furthermore, synchrotron-based measurements were carried out to reveal the underlying mechanism of MLD coating in Li–S batteries.

As shown in Figure 1, MLD process employs subsequent exposures of trimethylaluminum (TMA) and ethylene glycol

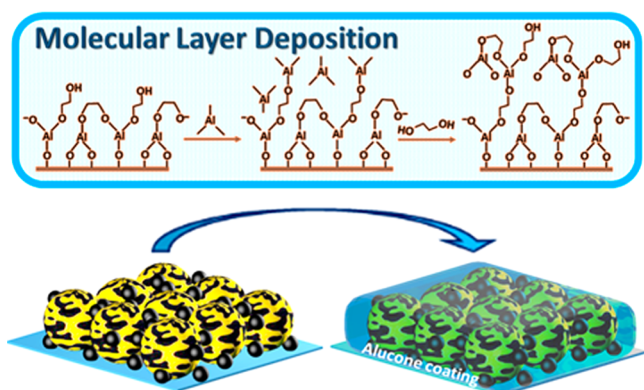


Figure 1. Schematic diagram of alucone coating on C–S electrode via molecular layer deposition.

(EG) into the reaction chamber to form a thin metal–organic coating on C–S electrodes. This reaction occurs in two half-reactions to form one monolayer of alucone (an inorganic–organic thin film composed of Al_2O_3 unit linked by $-\text{O}-\text{C}_2\text{H}_4-\text{O}-$ units), as shown in Figure 1. The thickness of the alucone coating can be precisely controlled by the number MLD cycles applied. In Figure 2a, SEM image demonstrates that the diameter of C–S particles in a 10-cycle alucone coated electrode ranges between 40 and 60 nm, which is close to that of the pristine C–S electrodes (Figure S1 and Figure S4). Elemental mapping using energy dispersive spectroscopy (EDS) reveals that the alucone coating is uniform along the surface of the film, as shown in Figure 2c and d. Furthermore,

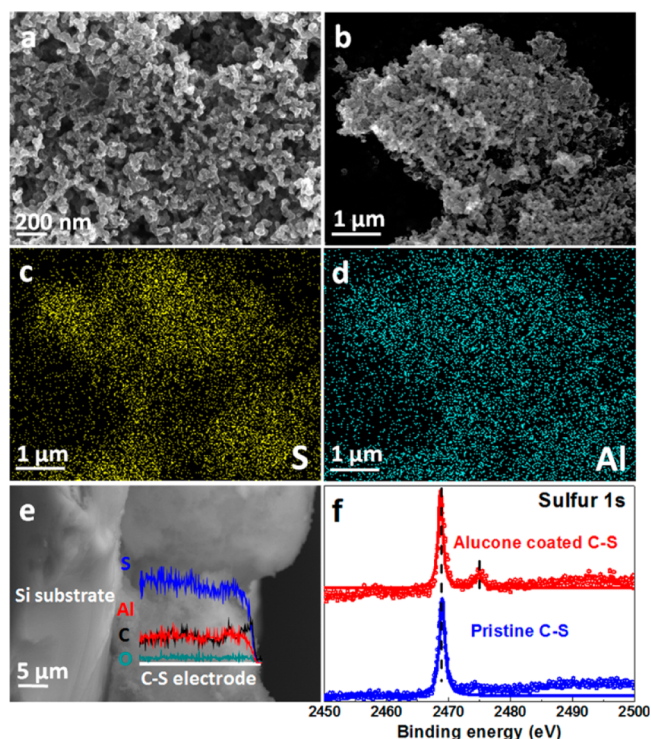


Figure 2. (a–b) FE-SEM images of alucone coated C–S electrode. (c–d) EDS elemental mapping profiles of b. (e) Linear-scanning EDS analysis of cross-section of alucone coated C–S electrode on silicon substrate. (f) Sulfur 1s HEXPS spectra of alucone coated and pristine C–S electrodes.

cross-sectional EDS analysis confirms that the MLD alucone film is also evenly distributed throughout the electrode vertically, demonstrating the conformal and uniform nature of the MLD process. Synchrotron based high energy X-ray photoelectron spectroscopy (HEXPS) further elucidates the interaction between sulfur and alucone coating. As shown in Figure 2f, compared to pristine C–S electrodes, the sulfur 1s spectrum for alucone coated electrode displays an additional peak at 2475.0 eV, demonstrating that very few of sulfur on the surface of electrode has interaction with alucone coating via S–O bond. Sulfur 1s spectra with different photo energies and Fourier transform infrared spectra (FTIR) were also conducted to further understand the interaction between alucone coating and sulfur, as shown in Figures S5 and S6. Thermogravimetric analysis result (TGA) demonstrates the sulfur load of carbon–sulfur composites as shown in Figure S3. The sulfur mass load of C–S composites is around 61 wt % after MLD process, and the sulfur areal loading of alucone coated C–S electrode is 0.9 mg cm^{-2} .

Electrochemical behavior of alucone coated and pristine C–S electrodes were evaluated using carbonate-based electrolyte (1 M LiPF_6 in ethylene carbonate (EC): ethyl–methyl carbonate (EMC): diethyl carbonate (DEC) solvents with 1:1:1 of volume ratio). Figure 3a displays the cycle performance of C–S electrodes under 0.1 C at room temperature (RT). Interestingly, alucone coated C–S electrodes exhibit dramatically improved performance in carbonate-based electrolyte compared to pristine electrodes. The alucone coated electrode shows an initial capacity of 912 mA h g^{-1} and stabilizes at 429 mA h g^{-1} after 100 cycles. In contrast, the pristine C–S electrode shows an initial discharge capacity of 940 mA h g^{-1} ;

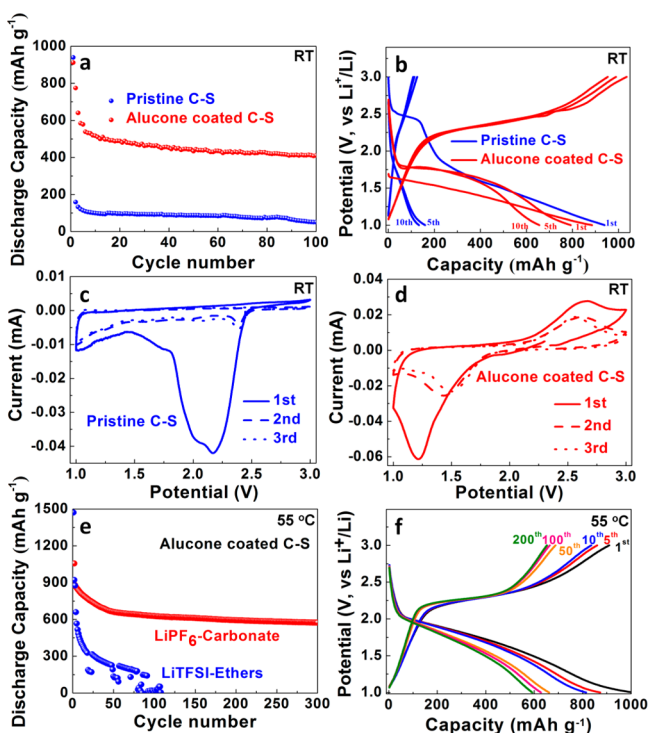


Figure 3. (a) Electrochemical cycle performance and (b) discharge–charge profiles of coated and pristine C–S electrode. Cyclic voltammograms profiles of (c) pristine C–S electrode and (d) coated C–S electrode. (e) Comparison of alucone coated C–S electrodes running within carbonate based and ether based electrolyte under 55 °C. (f) Discharge–charge profiles of alucone coated electrode operating in carbonate based electrolyte under 55 °C.

however, by the second cycle the discharge capacity significantly drops to 159 mA h g⁻¹, indicating irreversible electrochemical processes occurred, which is consistent with previous studies.^{6,15} Discharge–charge curves (Figure 3b) and corresponding cyclic voltammograms (CVs) (Figure 3c and d) provide further evidence that drastically different electrochemical processes had taken place in the coated and uncoated electrodes. In a typical Li–S battery where ether-based electrolyte is employed, two cathodic peaks at 2.3 and 2.1 V appear during the lithiated sulfur reaction, corresponding to the reduction of the S₈ molecule to long chain polysulfides and

then short chain sulfides in a two-step reaction; the anodic peak at 2.4 V corresponding to a reversed process, as shown in Figure S8.^{27–29} Interestingly, the pristine C–S electrode cycled in carbonate-based electrolytes displays a single broad cathodic peak at 2.5 V in the first cycle, and no peaks appeared in subsequent cycles. This type of behavior is indicative of long-chain polysulfides formation which may inhibit further electrochemical reaction.¹⁵ However, the alucone coated C–S electrode exhibits well-defined potential plateaus during the discharge and charge process, as well as reproducible cathodic and anodic peaks in the CV profile. Compared to typical Li–S redox reactions, alucone coated electrodes display a larger voltage gap between the cathodic and anodic peaks (1.5 and 2.5 V), representing an alternative reaction route as well as increased internal resistance.^{30,31} Electrochemical impedance spectra (EIS) were conducted to understand the influence of the MLD alucone coating layer on the conductivity of the electrode, as shown in Figure S10. The results indicate that the alucone coating layer maintains high activity toward electrochemical reactions for electrodes cycled in various electrolytes.

To demonstrate the electrochemical performance of the Li–S batteries at high temperature, the cycle stability of alucone coated C–S electrodes with both carbonate- and ether-based electrolytes were measured at 55 °C to simulate the environment for Li–S batteries in electric vehicles (Figure 3e). Impressively, alucone coated C–S demonstrates improved capacity and extended cycle life in Li–S batteries using carbonate-based electrolyte. Alucone coated electrodes exhibits an initial capacity of 1055 mA h g⁻¹, a value that exceeds the initial capacity conducted at room temperature. Elevated temperatures facilitate the diffusion of Li-ions and promote electrochemical reactions, resulting in improved battery performance.^{32,33} The capacity of the cell stabilizes at 661 mA h g⁻¹ after 50 cycles and with a capacity retention over 573 mA h g⁻¹ after 300 cycles, demonstrating extraordinary cycle life. Cyclic discharge–charge curves further demonstrate that the electrochemical processes taking place in alucone coated C–S electrodes operating at 55 °C is highly reversible. As shown in Figure 3f, potential plateaus in discharge and charge curves are stabilized at 2.0 and 2.3 V, displaying improved electrochemical activity at elevated temperature. For comparison, alucone coated C–S electrode was also cycled at 55 °C with ether-based electrolyte (1 M LiTFSI in dimethoxyethane (DME): dioxolane (DOL) with 1:1 of volume ratio), as

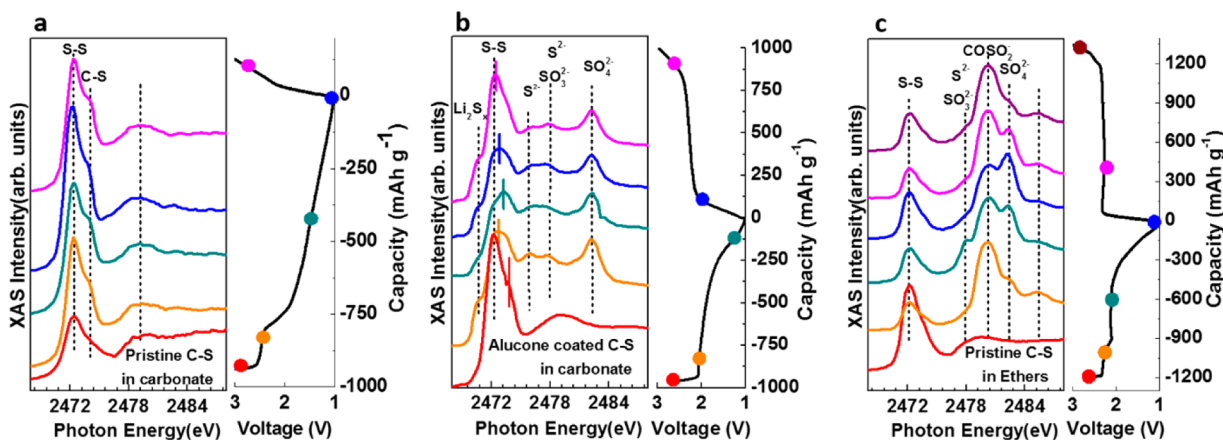


Figure 4. Sulfur K-edge spectra of C–S electrodes at discharge–charge steps. (a) Pristine C–S with carbonate based electrolyte; (b) alucone coated C–S with carbonate based electrolyte; and (c) pristine C–S with ether based electrolyte.

outlined in Figure 3e, which shows a rapid capacity decay with cell failure after 100 cycles. As mentioned earlier, the flash point of ether solvents DME and DOL is below 2 °C, which raises a number of safety issues for high temperature operation of Li–S batteries. Although 55 °C does not reach to boiling temperature of ether based electrolytes, this elevated temperature can still result in higher vapor pressure while also enhancing electrolyte consumption, bringing a number of deleterious effects into question.^{9–12} Based on these results, MLD alucone coating enables the use of secondary C–S cathodes in carbonate-based electrolyte and offers a safe and versatile approach toward Li–S batteries at elevated temperature.

Near edge X-ray absorption fine structure (NEXAFS) was conducted to further elucidate the mechanism behind the MLD alucone coating in C–S electrodes cycled in carbonate electrolyte. Figure 4 displays the S K-edge spectra for pristine C–S and alucone coated electrodes under discharge–charge steps to explore the chemical structure evolution of different electrodes. According to previous studies, the feature at 2472.2 eV can be attributed to the S 1s transition to S–S π^* state of elemental sulfur. Features located at 2476.2, 2478.0, 2480.5, and 2482.3 eV are assigned to the S 1s transition to Li_2S σ^* , S^{2-} σ^* , and/or SO_3^{2-} σ^* , COSO_2^- σ^* , and SO_4^{2-} σ^* , respectively.^{34,35} As shown in Figure 4a, pristine C–S electrodes during discharge–charge processes do not exhibit obvious peak shifts and only presents one new peak at 2474.0 eV. This additional peak most likely arises from side reactions occurring between long-chain polysulfides and carbonate-based solvents, producing $\text{S}_x\text{--C}_n\text{--C=O}^-$ species.^{15,36–38} It has been reported that this side reaction results in solvent decomposition which in turn hinders lithium ion diffusion.¹⁵ This observation, combined with the CV results, allows us to propose with confidence that the failure in uncoated C–S electrode in Li–S batteries with carbonate-based electrolytes can almost certainly be attributed to the reaction of long chain polysulfides with carbonate solvents. On the other hand, as shown in Figure 4b, the S K-edge spectra for alucone coated C–S electrodes show an interesting phenomenon. Prior to electrochemical testing, the NEXAFS spectra of the coated electrodes show an additional peak at 2473.6 eV assigned to C–S chemical bond, which indicates a chemical interaction between sulfur and alucone coating.³⁹ During the discharge–charge process, the S–S peak from alucone coated C–S electrode initially shifts from 2472.2 to 2473.4 eV, then returns to 2472.2 eV. This evolution is drastically different from the behavior of pristine C–S electrodes and is indicative of a reversible Li–S redox reaction occurring with the use of alucone coating.^{39,40} Previous literature results indicate that a shift in the S–S peak can be attributed to the transformation of elemental sulfur to polysulfides species, indicating an interaction between polysulfides and alucone coating layer.^{39–41} The final discharge product of the alucone coated C–S electrode (discharge 1.0 V) can be determined as Li_2S , as shown in Figure S13.^{41,42} XANES spectra of polysulfides S_n^{2-} exhibit a pre-edge peak at around 2470.2 eV along with a peak at 2472 eV. The Li_2S reference sample, on the other hand, only exhibits two peaks at 2470.8 and 2473.7 eV without any indication of a pre-edge peak. Compared to the reference sample, the spectra of alucone coated C–S electrode discharged to 1.0 V is in agreement with Li_2S , suggesting that sulfur can be reduced to Li_2S as the final discharge product in carbonate based electrolyte. Further, few SO_4^{2-} species are identified throughout the electrochemical

process, which is still an open question and most likely arises from the oxidation of sulfide species by alucone coating. From the comparison of Figure 4a with b, it is apparent that the major drawback for pristine C–S electrodes cycled in carbonate-based electrolytes is the occurrence of side reactions between long chain polysulfides and the surrounding carbonate solvents. From the S K-edge NEXAFS and the S 1s HEXPS spectra shown in Figure 2f, we propose that the alucone coating interacts with sulfur, further allowing the formation of few SO_4^{2-} species in electrochemical reactions, which ends up passivating the surface of the electrode and hindering unwanted side reaction. Therefore, the Li–S electrochemical process, along with the support of alucone coating, completes a solid-phase electrochemical reaction, leading to higher potential polarization during the electrochemical reactions at room temperature. Some pioneer research using “small sulfur” cathode also enabled a reversible electrochemical reaction in carbonate electrolyte, which also claimed “solid-phase” Li–S reaction and the discharge–charge curves in their paper are consistent with our results.¹⁷ Figure 4c shows the S K-edge spectra for pristine C–S electrodes in ether-based electrolyte as references and illustrates an alternative chemical structure evolution compared to sulfur cathodes cycled in carbonate-based electrolyte. During the discharge–charge process, the peak at 2472.2 eV does not shift, indicating that polysulfides are dissolved in ether-based electrolyte. Further, the COSO_2^- and SO_4^{2-} peaks exhibit a reversible tendency during discharge–charge process, which can be attributed to the presence of LiTFSI salt (Figure S14) and the oxidation of sulfide species.^{34,35} Comparison of Figure 4a with Figure 4b and c further demonstrates that a chemical interaction is taking place between the intermediate polysulfide species and alucone coating and confirms the solid-state Li–S redox reaction with the support of alucone coating in carbonate-based electrolyte.

In summary, we have shown that the MLD alucone coating is a novel and potentially universal approach which enables safe high temperature Li–S batteries with conventional carbon–sulfur electrodes. The MLD alucone coated C–S electrodes demonstrate stabilized ultralong cycle life at high temperature with a capacity over 570 mA h g⁻¹ after 300 cycles, representing the much stable and prolonged cycle performance for high-temperature Li–S batteries. The utilization of MLD enables the usage of conventional carbon–sulfur cathode materials for Li–S batteries with carbonate based electrolytes, which is a facile and versatile approach that can be applied to a variety of C–S electrodes without redesigning the carbon host materials. It should be noted that the current MLD alucone coated C–S electrodes in carbonate based electrolyte still presents a number of challenges and unsatisfactory cycle performance at room temperature. These issues are related to the limited conductivity of the MLD coating, the nanostructure of the carbon host, and the components of carbonate based solvents. Our future work is aimed at further improving these portions of the Li–S batteries.

■ ASSOCIATED CONTENT

Supporting Information

The Supporting Information is available free of charge on the ACS Publications website at DOI: 10.1021/acs.nanolett.6b00577.

Experimental details and additional physical and electrochemical characterization (PDF)

AUTHOR INFORMATION

Corresponding Author

*E-mail: xsun9@uwo.ca.

Present Addresses

W.X., B.W., and T.-K.S.: Department of Chemistry, University of Western Ontario, ON, N6A 5B9, Canada.

Y.Y.: National Synchrotron Radiation Laboratory, University of Science and Technology of China, Hefei, 230029, China.

K.N.: Soochow University-Western University Centre for Synchrotron Radiation Research, Institute of Functional Nano and Soft Material (FUNSOM), Soochow University, Suzhou, 215123, China.

Notes

The authors declare no competing financial interest.

ACKNOWLEDGMENTS

This research was supported by Natural Sciences and Engineering Research Council of Canada (NSERC), Canada Research Chair Program (CRC), Canada Foundation for Innovation (CFI), Ontario Research Fund, the Canada Light Source at University of Saskatchewan (CLS), and the University of Western Ontario. The Advanced Light Source is supported by the Director, Office of Science, Office of Basic Energy Sciences, of the U.S. Department of Energy under Contract No. DE-AC02-05CH11231. Y.Y. and K.N. acknowledge Prof. Junfa Zhu (University of Science and Technology, China) and Prof. Xuhui Sun's supervision (Soochow University, China), respectively and for their support of this study. Dr. Jian Liu is grateful to the financial support from NSERC Postdoctoral Fellowship Program.

REFERENCES

- Bruce, P. G.; Freunberger, S. A.; Hardwick, L. J.; Tarascon, J. M. *Nat. Mater.* **2011**, *11*, 19–29.
- Gao, X.-P.; Yang, H.-X. *Energy Environ. Sci.* **2010**, *3*, 174–189.
- Lu, L.; Han, X.; Li, J.; Hua, J.; Ouyang, M. *J. Power Sources* **2013**, *226*, 272–288.
- Barré, A.; Deguilhem, B.; Grolleau, S.; Gérard, M.; Suard, F.; Riu, D. *J. Power Sources* **2013**, *241*, 680–689.
- Aurbach, D.; Pollak, E.; Elazari, R.; Salitra, G.; Kelley, C. S.; Affinito, J. *J. Electrochem. Soc.* **2009**, *156*, A694–A702.
- Zhang, S. S. *Electrochim. Acta* **2012**, *70*, 344–348.
- Wang, H.; Yang, Y.; Liang, Y.; Robinson, J. T.; Li, Y.; Jackson, A.; Cui, Y.; Dai, H. *Nano Lett.* **2011**, *11*, 2644–7.
- Zheng, G.; Yang, Y.; Cha, J. J.; Hong, S. S.; Cui, Y. *Nano Lett.* **2011**, *11*, 4462–7.
- Gordin, M. L.; Dai, F.; Chen, S.; Xu, T.; Song, J.; Tang, D.; Azimi, N.; Zhang, Z.; Wang, D. *ACS Appl. Mater. Interfaces* **2014**, *6*, 8006–10.
- Busche, M. R.; Adelhelm, P.; Sommer, H.; Schneider, H.; Leitner, K.; Janek, J. *J. Power Sources* **2014**, *259*, 289–299.
- Kim, H.; Lee, J. T.; Yushin, G. *J. Power Sources* **2013**, *226*, 256–265.
- Huang, J.-Q.; Liu, X.-F.; Zhang, Q.; Chen, C.-M.; Zhao, M.-Q.; Zhang, S.-M.; Zhu, W.; Qian, W.-Z.; Wei, F. *Nano Energy* **2013**, *2*, 314–321.
- Zhang, S. S. *J. Power Sources* **2013**, *231*, 153–162.
- Barchasz, C.; Leprêtre, J.-C.; Patoux, S.; Alloin, F. *Electrochim. Acta* **2013**, *89*, 737–743.
- Yim, T.; Park, M.-S.; Yu, J.-S.; Kim, K. J.; Im, K. Y.; Kim, J.-H.; Jeong, G.; Jo, Y. N.; Woo, S.-G.; Kang, K. S.; Lee, I.; Kim, Y.-J. *Electrochim. Acta* **2013**, *107*, 454–460.
- Zhang, B.; Qin, X.; Li, G. R.; Gao, X. P. *Energy Environ. Sci.* **2010**, *3*, 1531–1537.
- Xin, S.; Gu, L.; Zhao, N. H.; Yin, Y. X.; Zhou, L. J.; Guo, Y. G.; Wan, L. J. *J. Am. Chem. Soc.* **2012**, *134*, 18510–18513.
- Meng, X.; Yang, X. Q.; Sun, X. *Adv. Mater.* **2012**, *24*, 3589–3615.
- Zhou, H.; Bent, S. F. *J. Vac. Sci. Technol., A* **2013**, *31*, 040801.
- Dameron, A. A.; Seghete, D.; Burton, B. B.; Davidson, S. D.; Cavanagh, A. S.; Bertrand, J. A.; George, S. M. *Chem. Mater.* **2008**, *20*, 3315–3326.
- Liu, J.; Sun, X. *Nanotechnology* **2015**, *26*, 024001.
- Li, X.; Meng, X.; Liu, J.; Geng, D.; Zhang, Y.; Banis, M. N.; Li, Y.; Yang, J.; Li, R.; Sun, X.; Cai, M.; Verbrugge, M. W. *Adv. Funct. Mater.* **2012**, *22*, 1647–1654.
- Lee, B. H.; Yoon, B.; Anderson, V. R.; George, S. M. *J. Phys. Chem. C* **2012**, *116*, 3250–3257.
- Li, X.; Lushington, A.; Liu, J.; Li, R.; Sun, X. *Chem. Commun.* **2014**, *50*, 9757–60.
- Kim, H.; Lee, J. T.; Lee, D.-C.; Magasinski, A.; Cho, W.-i.; Yushin, G. *Adv. Energy Mater.* **2013**, *3*, 1308–1315.
- Han, X.; Xu, Y.; Chen, X.; Chen, Y.-C.; Weadock, N.; Wan, J.; Zhu, H.; Liu, Y.; Li, H.; Rubloff, G.; Wang, C.; Hu, L. *Nano Energy* **2013**, *2*, 1197–1206.
- Evers, S.; Nazar, L. F. *Acc. Chem. Res.* **2013**, *46*, 1135–1143.
- Elazari, R.; Salitra, G.; Garsuch, A.; Panchenko, A.; Aurbach, D. *Adv. Mater.* **2011**, *23*, 5641–5644.
- Pu, X.; Yang, G.; Yu, C. *Adv. Mater.* **2014**, *26*, 7456–7641.
- Nagao, M.; Hayashi, A.; Tatsumisago, M. *Electrochim. Acta* **2011**, *56*, 6055–6059.
- Nagao, M.; Imade, Y.; Narisawa, H.; Kobayashi, T.; Watanabe, R.; Yokoi, T.; Tatsumi, T.; Kanno, R. *J. Power Sources* **2013**, *222*, 237–242.
- Lin, Z.; Liu, Z.; Fu, W.; Dudney, N. J.; Liang, C. *Angew. Chem., Int. Ed.* **2013**, *52*, 7460–3.
- Lin, Z.; Liang, C. *J. Mater. Chem. A* **2015**, *3*, 936–958.
- Lin, Z.; Nan, C.; Ye, Y.; Guo, J.; Zhu, J.; Cairns, E. *J. Nano Energy* **2014**, *9*, 408–416.
- Feng, X.; Song, M. K.; Stolte, W. C.; Gardenghi, D.; Zhang, D.; Sun, X.; Zhu, J.; Cairns, E. J.; Guo, J. *Phys. Chem. Chem. Phys.* **2014**, *16*, 16931–16940.
- Vijayakumar, M.; Govind, N.; Walter, E.; Burton, S. D.; Shukla, A.; Devaraj, A.; Xiao, J.; Liu, J.; Wang, C.; Karim, A.; Thevuthasan, S. *Phys. Chem. Chem. Phys.* **2014**, *16*, 10923–10932.
- Fu, C.; Wong, B. M.; Bozhilov, K. N.; Guo, J. *Chem. Sci.* **2016**, *7*, 1224–1232.
- Cuisinier, M.; Hart, C.; Balasubramanian, M.; Garsuch, A.; Nazar, L. F. *Adv. Energy Mater.* **2015**, *5*, 1401801.
- Jalilehvand, F. *Chem. Soc. Rev.* **2006**, *35*, 1256–1268.
- Vairavamurthy, A. *Spectrochim. Acta, Part A* **1998**, *54*, 2009–2017.
- Patel, M. U.; Arcon, I.; Aquilanti, G.; Stievano, L.; Mali, G.; Dominko, R. *ChemPhysChem* **2014**, *15*, 894–904.
- Cuisinier, M.; Cabelguen, P.-E.; Evers, S.; He, G.; Kolbeck, M.; Garsuch, A.; Bolin, T.; Balasubramanian, M.; Nazar, L. F. *J. Phys. Chem. Lett.* **2013**, *4*, 3227–3232.